AIAA JOURNAL
Vol. 30, No. 5, May 1992

Nonlinear Damping Estimation from Rotor Stability Data Using Time and Frequency Domain Techniques

Frederick Tasker* and Inderjit Chopra†
University of Maryland, College Park, Maryland 20742

For estimating equivalent damping characteristics from transient response data involving nonlinear damping, modifications to two stability testing methods, the moving-block technique and the sparse time domain method, are presented and verified by the use of numerical simulations. Effects of large undamped response and noise on the performance of these techniques are evaluated for quadratic and coulomb dampings. It is concluded that equivalent damping characteristics may be identified from sampled, multimode and noisy nonlinear transient response data using modified versions of the moving-block analysis and the sparse time domain method.

Nomenclature

A = initial amplitude of free decay response
$a(t)$ = instantaneous amplitude of free decay response
a_k = real part of discrete Fourier transform at kth harmonic
b = vector of backward prediction coefficients
b_k = imaginary part of discrete Fourier transform at kth harmonic
$F(\omega,\tau)$ = moving-block function
H = upper Hessenberg system matrix
M = number of rows in data matrix
N = number of assumed modes in response
N_b = number of samples in discrete Fourier transform
T = time duration of block
U = $M \times M$ matrix of left singular vectors
V = $2N \times 2N$ matrix of right singular vectors
$x(t)$ = vector of responses at time t
α = diagonal matrix of eigenvalues in exponential form
ϵ = coefficient of quadratic damping
ζ = viscous damping ratio
$\zeta_{eq}(t)$ = equivalent viscous damping ratio
Λ = Vandermode signal matrix
λ_i = eigenvalue of ith mode
$\lambda_{eq}(t)$ = instantaneous value of decay coefficient
μ = coulomb damping force
ω = frequency, rad/s
Σ = matrix of singular values
σ = singular value
τ = time origin of data block
Φ = data matrix
Ψ = modal matrix

Introduction

THE aeroelastic stability of a helicopter rotor is determined by the coupling of complex aerodynamic, structural, and inertial forces. It is well recognized that nonlinear effects are quite important in rotor stability phenomena. In a rotor stability test, typically a few transient response records at a particular trim setting are taken. The stability data often exhibit large scatter, partially attributed to nonlinear damping characteristics. Because of the high cost and safety hazards involved with wind-tunnel testing of rotor models, stability testing is generally performed under strict time constraints. This means that experiments cannot be repeated a sufficient number of times to ensure reliable averaging. Also, the presence of close modes, low signal-to-noise ratios, impulsive forcing due to stalled flows, and the rotating environment further aggravates the identification of damping characteristics. The task of estimating the damping of any mode for a rotor model is further complicated by the presence of substantial amplitudes of harmonics of the rotational speed. Furthermore, it is quite difficult to excite a mode in the rotating environment. It is therefore a challenging task to identify damping and frequency from the response data.

A good example of the difficulties associated with rotor stability testing is the survey conducted by Warmbrodt.[1] In this survey, several major helicopter companies were asked to determine damping from the same transient response data. The data were collected from the stability testing of helicopter rotor models in wind tunnels. It was interesting that each company, using their own analysis techniques, came up with different estimates for the low-frequency, low damped chordwise mode damping. It could not be concluded which one of the techniques yielded better estimates. If a stability analysis is to be validated through the correlations of calculated and measured results, then it is essential that the damping of modes must be identified accurately from measured response data.

In a transient test, one approach is to give an impulsive motion to a blade through the pitch-control system, and then record the subsequent free decay response from a pickup mounted on the blade. Another approach is to excite the blade at a discrete frequency through the pitch-actuation system and then impulsively cut off the sinusoidal forcing for the free response. In the rotating environment, the second approach is generally adopted. It also can help to identify higher modes. The recorded transient response data are then analyzed by one of various techniques. Transient techniques are usually preferred for rotor stability because of the minimal amount of instrumentation and data record needed, and also they require less test time.

A number of techniques exists in the literature for detection, characterization, and identification of nonlinearities (a survey of this topic is given in Ref. 2). Detection methods include monitoring of parametric changes with force levels, reciprocity checks, Hilbert transform operations, polyspectral analysis, and Kennedy-Pancu plots. Some of these methods may also be used to characterize nonlinearities. For example, Nayfeh[3] suggested several types of experiments based on parametric variations to characterize nonlinear behavior, and Lai[4] discussed

Presented as Paper 89-1243 at the AIAA/ASME/ASCE/AHS 30th Structures, Structural Dynamics, and Materials Conference, Mobile, AL, April 3-5, 1989; received Aug. 14, 1990; revision received July 15, 1991; accepted for publication Sept. 7, 1991.

*Graduate Research Assistant; currently, Assistant Professor, Mechanical Engineering, University of Maryland-UMBC, Baltimore, MD 21228. Member AIAA.

†Professor of Aerospace Engineering. Fellow AIAA.

the use of polyspectra and higher-order statistical moments, such as skewness and kurtosis, for detecting quadratic and cubic nonlinearities.

Identification of a nonlinear system may be parametric or nonparametric. Parametric identification proceeds from a well-defined model having unknown parameters. This model may be obtained from the physics of the system, or as a result of an extensive characterization study.[3,4] Well-known techniques for determining the unknown parameters include nonlinear least squares,[5] extended Kalman filtering,[6] and nonlinear regression models that are linear in the parameters.[4,7]

In nonparametric identification, the model is more general (and usually less parsimonious) to account for the lack of prior information. This method is not based on the physics of the system that is being identified. A common example is a discrete Fourier transform, which is a nonparametric representation of a time series in terms of a set of sine and cosine functions. Another nonparametric method for identification involves the use of Volterra and Weiner kernels; these are, however, prohibitively expensive to use. Masri and Caughey[8] expanded the nonlinear restoring force of a single-degree-of-freedom system in terms of Chebyshev polynomials. This is a force-state mapping technique. Udwadia and Kuo[9] generalized this method to multi-degree-of-freedom systems and also incorporated other orthogonal polynomials. These methods make use of velocity and displacement measurements that may be obtained by integrating acceleration measurements. However, accelerations cannot be easily measured in a helicopter rotor stability test. Hadjian et al.[10] has given a review of methods for calculating equivalent damping from nonlinearly damped systems. Transient methods that are frequently used for the estimation of equivalent damping are better suited to the analysis of single-degree-of-freedom analog response. Such methods are not well suited to multimode, noise corrupted, sampled data. In the present paper, improved digital transient data analysis techniques are used. These enable good estimation of parameters from short segments of data. It is then possible to obtain better "instantaneous" linear estimates from multimode, noisy transient response data, which are representative of rotor stability data.

The moving-block technique[11,12] is the most commonly used stability measurement approach in the rotorcraft industry. It is a simple technique and can be easily implemented for on-line data analysis. The authors[13] introduced several modifications in this technique in order to make it efficient and accurate for the analysis of rotor stability data. This modified method was successfully applied in an on-line stability analysis of a model bearingless rotor in the Glenn L. Martin wind tunnel at the University of Maryland.[14]

Another transient stability measurement approach is the sparse time domain (STD) technique,[15] a modified version of the Ibrahim time domain (ITD) approach. The ITD approach has been applied to a wide variety of test structures and has been found to be an accurate technique to identifiy modal characteristics. It is implemented by forming two response matrices, one being the reference matrix and the other the shifted matrix in time. The natural frequencies and damping of various modes of the test structure can be obtained from an eigenanalysis of the system matrix formed from these two matrices. In the sparse time domain method, the system matrix is reduced to the upper Hessenberg form, which substantially simplifies the computation of the eigenvalues. Furthermore, the application of a singular value decomposition solution to this technique causes a reduction in the variance of the estimated parameters.[13,16] The application of this scheme to a recent stability test of a bearingless rotor revealed that the computational time needed to reduce data was quite substantial. To overcome this problem, the eigenvalue problem was modified to compute only the structural modes from the overdetermined system matrices. It was accomplished by using the method of simultaneous vector iteration for unsymmetrical matrices that helped to reduce computation time. In fact, one is able to obtain reduced variance estimates with negligible increase in computation time.

This paper discusses the application of these two techniques, moving-block and modified STD, to the estimation of nonlinear damping characteristics in the rotating environment. Two nonlinear damping models, quadratic and coulomb damping, are studied through numerical simulations. The effects of several parameters on damping identification are examined, including noise level, content of close harmonics, data length, and block size.

Moving-Block Analysis

The finite Fourier transform of a damped sinusoid is given by

$$F(\omega,\tau) = \int_{\tau}^{T+\tau} Ae^{-\zeta\omega_n t}\sin(\omega_d t+\phi)e^{-i\omega t}\,dt \tag{1}$$

where ω_n is the natural frequency, ω_d is the damped natural frequency, and T is the record length. The natural logarithm of the moving-block function $F(\omega,\tau)$ may be evaluated approximately at $\omega=\omega_n\approx\omega_d$ and for $\zeta\ll 1.0$ to give

$$\ell n|F(\omega_n,\tau)| = -\zeta\omega_n\tau + \ell n(A/2\omega_n) + \tfrac{1}{2}\ell n\left[\frac{1+f(\zeta,\tau,T)}{\zeta^2}\right] \tag{2}$$

where

$$\begin{aligned} f(\zeta,\tau,T) = {} & -2e^{-\zeta\omega_n T} + e^{-2\zeta\omega_n T} \\ & + (1-e^{-\zeta\omega_n T})\zeta\sin(2\omega_n\tau+2\phi) \\ & - e^{-\zeta\omega_n T}(1-e^{\zeta\omega_n T})\left\{\zeta\sin\left[2\omega_n(\tau+T)+\phi\right]\right\} \end{aligned} \tag{3}$$

This implies that the plot of $\ell n|F(\omega_n,\tau)|$ against τ would be a straight line of slope $-\zeta\omega_n$ with a superimposed oscillatory part of frequency $2\omega_n$.

A moving-block implementation consists of calculating the natural logarithm of the amplitude of the spectrum at a specified frequency, and then shifting the origin of the data block for subsequent times. A straight line is then fitted to the resulting logarithmic plot of amplitudes with time.

The calculation of the spectral amplitude at the frequency of interest can be accomplished by two methods. The first is to use the fast Fourier transform (FFT) algorithm and then move the origin of the transform block. This method, although very efficient, calculates the spectrum at more frequencies than needed. Another method is to use the direct truncated Fourier transform at the specified frequency, but this is time consuming. A better and efficient approach is to use Hamming's local Fourier series solution[12,13] that significantly cuts down on the computation time. It is a recursive technique for calculating the Fourier coefficients for slowly time-varying signals.

Following Hamming's derivation,[17] the Fourier coefficients at time $(\tau+1)$ can be shown to be

$$\begin{aligned} a_k(\tau+1) = {} & a_k(\tau)\cos(2\pi k/N_b) + b_k(\tau)\sin(2\pi k/N_b) \\ & + (2/N_b)\left\{x(N_b+\tau)\cos\left[2\pi k(N_b-1)/N_b\right]\right. \\ & \left. - x(\tau)\cos(2\pi k/N_b)\right\} \end{aligned} \tag{4}$$

$$\begin{aligned} b_k(\tau+1) = {} & b_k(\tau)\cos(2\pi k/N_b) - a_k(\tau)\sin(2\pi k/N_b) \\ & + (2/N_b)\left\{x(N_b+\tau)\sin\left[2\pi k(N_b-1)/N_b\right]\right. \\ & \left. + x(\tau)\sin(2\pi k/N_b)\right\} \end{aligned} \tag{5}$$

These reduce to the results of Ref. 17 when k is an integer. The preceding form is more general since it can also handle noninteger harmonics. This is useful because the estimated

damping ratio is sensitive to the frequency at which the analysis is performed.[12] Also,

$$\ell n|F(\omega,\tau)| = 0.5\,\ell n\left[a_k^2(\tau)+b_k^2(\tau)\right] \tag{6}$$

One major concern with the use of the moving-block method for analysis with close modes is leakage.[12] Leakage occurs when the signal to be transformed is truncated. This is equivalent to multiplying the signal with a boxcar window. This multiplication corresponds to the convolution of the spectra of the boxcar window with that of the signal. Energy is said to have leaked from the frequency of interest to other frequencies. It was concluded in Ref. 12 that the use of the Hanning window offers significant improvements in the estimation of the damping of close modes by the moving-block method. Its use, however, was hampered by the substantial increase in computation time resulting from the recursive formula given by Eqs. (4) and (5) not being valid when the data are multiplied by a window function. It then becomes necessary to calculate the moving-block function by the direct truncated Fourier transform, and this can be substantially slower (typically about 30 times) than the recursive technique without windowing. In Ref. 13, the authors modified the recursive formula for a Hanning window. This leads to computation times quite comparable to moving-block analysis done without a window.

The damping ratio is usually obtained from the natural logarithm of the moving-block function by fitting a least-squares line to a selected part of the data. In a rotor system, there are two sources of damping—structural and aerodynamic. A blade undergoing coupled motion in forward flight is exposed to a complex aerodynamic environment which results in a nonlinearly damped system. Depending on the flight condition, these nonlinearities may be significant. It is of interest to know the actual damping behavior of the system before it is averaged out by the processing algorithms.

In this paper, the moving-block analysis technique is adapted to process small blocks of data in order to obtain the detailed damping variation with amplitude. The damping is determined in terms of an equivalent viscous damping. The equivalent damping at various times is determined from the slope of short intervals of the logarithm of amplitude plot. The factors that critically affect the performance of this technique are then studied.

Sparse Time Domain Technique

The STD technique is a multiple output, multi-degree-of-freedom technique for estimating the modal parameters from transient response data.[15] This technique may be considered as an extended Prony method for multi-output data.

The free response of a viscously damped lumped parameter system may be written as

$$\{x(t)\} = \sum_{j=1}^{2N} \{\psi_j\} e^{\lambda_j t} \tag{7}$$

where ψ_j is the jth mode shape and λ_j is the jth eigenvalue,

$$\lambda_j = -\zeta_j\omega_j + i\omega_j\sqrt{1-\zeta_j^2} \tag{8}$$

ζ_j is the damping ratio of jth mode and ω_j is its natural frequency. Equation (7) may be written at different time instants as

$$\left[x(t_1), x(t_2), \ldots, x(t_{2N})\right] = \left[\psi_1, \psi_2, \ldots, \psi_{2N}\right][\Lambda]$$

where $\Lambda_{ij} = e^{\lambda_i t_j}$. These may be written as

$$[\Phi] = [\Psi][\Lambda] \tag{9}$$

If the response matrix is shifted by Δt, then Eq. (9) becomes

$$[\hat{\Phi}] = [\Psi][\hat{\Lambda}] \tag{10}$$

where

$$[\hat{\Lambda}] = [\alpha][\Lambda] \tag{11}$$

and $\alpha_{ii} = e^{\lambda_i \Delta t}$ which leads to

$$[\hat{\Phi}][\Lambda]^{-1} = [\Phi][\Lambda]^{-1}[\alpha] \tag{12}$$

and

$$[H][\Lambda]^{-1} = [\Lambda]^{-1}[\alpha] \tag{13}$$

$[H]$ is the solution of $[\Phi][H] = [\hat{\Phi}]$ and Eq. (13) is its eigenvalue/eigenvector decomposition. From the structure of $[\Phi]$ and $[\hat{\Phi}]$, $[H]$ is an upper Hessenberg matrix[15] and only its last column contains useful information. All other elements of this matrix are zero with the exception of entries on the lower diagonal which are unity. Solving for the last column of $[H]$ leads to

$$[\Phi]\{a\} = \{\hat{\phi}_{2N}\} \tag{14}$$

where $\{\hat{\phi}_{2N}\}$ is the last column of $[\hat{\Phi}]$. From Eq. (13), the eigenvalues of $[H]$ are $e^{\lambda_i \Delta t}$ and the eigenvectors are the columns of $[\Lambda]^{-1}$. Using Eq. (8), the natural frequency and damping factor of each mode may be obtained from its eigenvalue, and the mode shape may be determined using Eq. (9).

Equation (14) can be written for a single response location by the use of pseudostations[15] which are the actual response locations delayed in time. This leads to

$$\begin{bmatrix} x(1+2Nl) & \cdots & x(1+l) \\ x(1+2Nl+p) & \cdots & \cdots \\ \vdots & \ddots & \vdots \\ x\left[1+2Nl+(M-1)p\right] & & x\left[1+l+(M-1)p\right] \end{bmatrix} \begin{Bmatrix} a_1 \\ \vdots \\ \vdots \\ a_L \end{Bmatrix} = \begin{Bmatrix} x(1) \\ \vdots \\ \vdots \\ x\left[1+(M-1)p\right] \end{Bmatrix} \tag{15}$$

where l is the number of sampling intervals between columns in the data matrix, and p is the number of sampling intervals between rows. It turns out that the preceding linear prediction type of equations occur in a variety of fields, and different computational techniques have been utilized to solve them. These equations are in the backward prediction format. The use of the singular value decomposition (SVD) procedure for the solution of these equations involving damped signals and noise was demonstrated in Ref. 16. It was observed that the backward prediction arrangement caused the signal eigenvalues to fall outside the unit circle whereas the extraneous modes remained within it. This is desirable in the identification of the primary modes of the response signals, from those due to noise. Singular value decomposition extends this favorable eigenvalue arrangement to high noise levels and also reduces the variance of estimated frequencies. The use of SVD with backward prediction was applied in Ref. 13 for the estimation of the damping value of exponentially (linearly) damped sinusoids in the presence of large undamped responses and noise. This example is of particular interest to rotary wing stability testing.

The SDV of the data matrix in Eq. (14) is given as

$$[\Phi] = [U][\Sigma][V]^T \tag{16}$$

where Σ is a diagonal matrix ($M \times 2N$) with the singular values arranged in descending order. In the case where the data are

not contaminated with noise, the rank of [Φ] would be exactly equal to twice the number of structural modes present in the data. With the presence of noise, the matrix is of full rank. The solution of the matrix equation becomes

$$\{b\} = [V][\Sigma]^{+}[U]^{T}\{\hat{\phi}_1\} \tag{17}$$

To obtain $[\Sigma]^{+}$, all of the singular values corresponding to the noise subspace are set to zero. This procedure removes the contribution of the noise subspace eigenvectors from the solution of the equations. In other words, the columns of U and V corresponding to the deleted singular values do not participate in the solution. Application of this technique to rotor stability testing has shown the need to increase the computational efficiency.

It is unnecessary to compute all the eigenvalues of $[H]$. By using the backward prediction technique, the structural modes fall outside the unit circle, whereas the noise-related modes are constrained to remain inside it by the SVD solution. This means that the structural modes have the largest eigenvalue magnitudes. A simultaneous vector iteration scheme[18] for unsymmetric matrices is then used to compute the largest eigenvalues. This method consists of a premultiplication stage in which a trial set of vectors are multiplied with the matrix and a reorientation stage in which an interaction matrix is calculated and its eigensolution is obtained. Convergence of the partial eigensolution terminates the procedure. The speed of convergence of this method is, however, dependent on the separation of the computed eigenvalues from the other eigenvalues of the matrix. Although the $[H]$ matrix is very sparse, and therefore ideal for iterative methods, it was found that the small separation of eigenvalues caused very slow convergence times. For example, a typical spread of the eigenvalue magnitudes for structural modes at 9, 7, and 5 Hz, all with 1% damping and a sampling frequency of 20 Hz, would be 1.0287, 1.0222, and 1.016, and the extraneous modes would typically have magnitudes ranging from 0.98–0.9. A simple technique to improve convergence is to begin the iterations using the right singular vectors $[V]$ obtained in the solution of the linear prediction equations. This method was found to give rapid convergence to the partial eigensolution. The implication of fast solution of the eigevalue problem is that higher orders of the data matrices may be used, resulting in improved damping estimates.

Application of this method will help to determine the nonlinear damping characteristics by using short durations of the transient response data. This short time window is then moved across the data to calculate damping for all times.

Simulation Results

Consider a linearly damped response

$$x(t) = e^{-\zeta\omega_n t}\sin(\omega_d t + \phi) \tag{18}$$

where $\omega_n = 2\pi \times 9$ rad/s and $\zeta = 0.01$. The data set was generated with a sampling frequency of 409.6 Hz. Figure 1a shows the estimated damping as a function of time, calculated using the moving-block analysis with short intervals of the moving-block function. The block size used to compute the moving-block function is 50 samples and the local damping is determined by fitting a curve to a small set of points contained in one period of the frequency of interest (1/9 s). This shows that even for a linear damping case, the use of short intervals of the moving-block function deteriorates the damping estimates because of the superimposed oscillations that occur at twice the frequency of analysis. These oscillations are particularly severe if the Hanning window is not used. An increase in block size from 50–100 samples gives a better estimate of damping as shown in Fig. 1b. This illustrates that the oscillations are considerably reduced by using a large block size. This can also be deduced from Eq. (3) by making T large. The use of a Hanning window improves the damping estimates for both block sizes. It is therefore important to use the Hanning window for the implementation of moving-block analysis with a small block size. This is especially recommended since the windowing in moving-block analysis is amenable to recursive computation.[13] Subsequent results are obtained with a Hanning window.

The performance of the short-period moving-block analysis when applied to a response with quadratic damping is shown in Figs. 2a and 2b, respectively, for block sizes of 100 and 200. The calculated damping value typically represents an average value for the data block. Therefore, there is a choice of time assignment for the instantaneous damping. In the present figures, two time assignments are shown, one at the middle of the data block and the other at the end of data block. For simulation, the response is generated numerically by integrating the following differential equation:

$$\ddot{x} + \epsilon|\dot{x}|\dot{x} + \omega_n^2 x = 0 \tag{19}$$

In the simulations, $\epsilon = 0.005$ is used. The analytical values of equivalent damping at different times are generated by the method of equivalent linearization,[20] which is also known as the method of slowly varying amplitude and phase. Assume the response of the system as

$$x(t) = a(t)\sin\left[\omega_n t + \beta(t)\right] \tag{20}$$

Then with the assumption that within a time period $(2\pi/\omega_n)$ the amplitude and phase are approximately constant, it can be shown for quadratic damping that

$$\dot{a}(t) = \left[-4\epsilon a(t)\omega_n/3\pi\right]a(t) \tag{21}$$

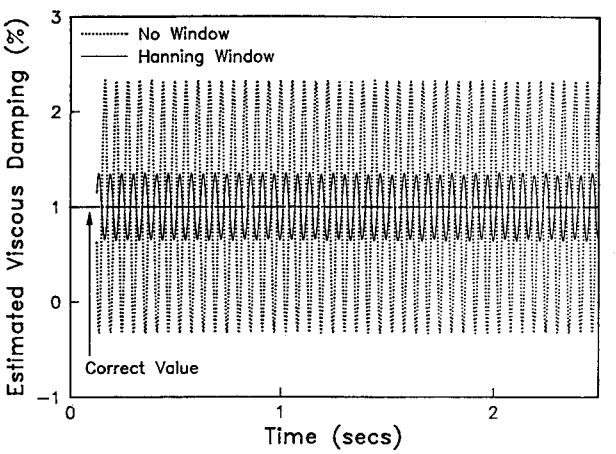

Fig. 1a Equivalent damping estimation using moving-block analysis (block size = 50, viscous damping $\zeta = 0.01$, frequency = 9 Hz).

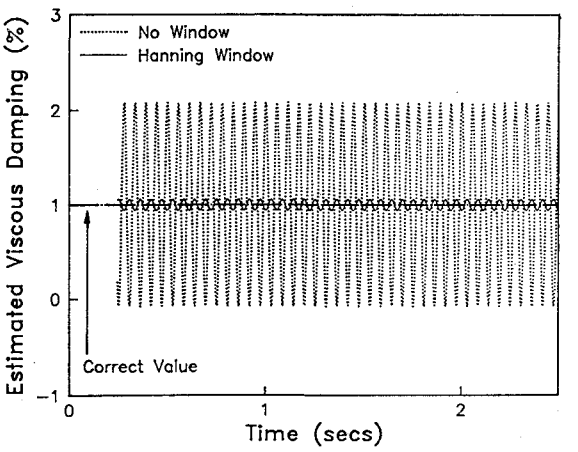

Fig. 1b Equivalent damping estimation using moving-block analysis (block size = 100, viscous damping $\zeta = 0.01$, frequency = 9 Hz).

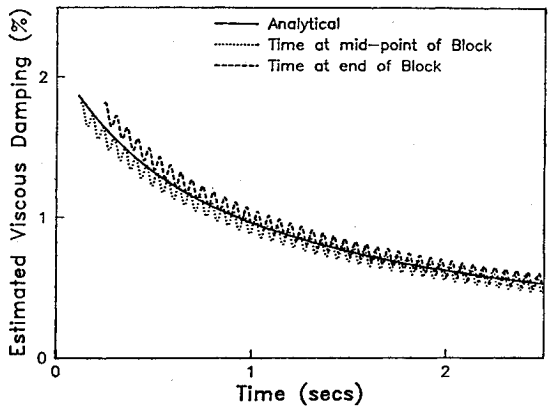

Fig. 2a Equivalent damping estimates for quadratic damping using moving-block analysis (block size = 100, analysis frequency = 9 Hz).

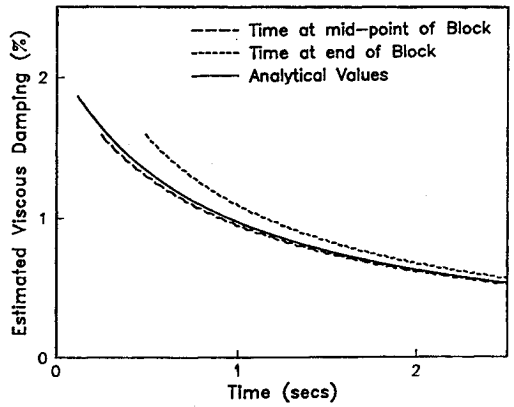

Fig. 2b Equivalent damping estimates for quadratic damping using moving-block analysis (block size = 200, analysis frequency = 9 Hz).

$$\dot{a}(t) = \lambda_{eq}(t)a(t) = -\omega_n \zeta_{eq}(t)a(t) \tag{22}$$

The solution of Eq. (21) is

$$a(t) = 3\pi a(0)/\left[3\pi + 4\epsilon\omega_n a(0)t\right] \tag{23}$$

which gives

$$\zeta_{eq}(t) = (4/3\pi)\epsilon a(t) = 4\epsilon a(0)/\left[3\pi + 4\epsilon\omega_n a(0)t\right] \tag{24}$$

It can be seen that the moving-block method gives a good description of the damping mechanism in spite of the small block size used (100 samples). The superimposed oscillations are small. The effect of using a finite block size to evaluate the envelope, and hence the damping, occurs at the beginning of the analysis where details may be missing due to averaging over the length of the block. To make a comparison with the analytical values, it is important to correctly assign a time value to each damping estimate. Usually the time assigned to an estimate is the time of the last datum used in obtaining that estimate[21] (i.e., the end point of block size). From the figures, it is quite clear that the damping estimation is represented better if the time is assigned to the midpoint of the block size. Again, the damping estimation improves with a larger block size.

Results obtained using the STD analysis for the same quadratic damping response are shown in Fig. 3. This shows that in spite of using a smaller number of samples (48 samples), the character of the damping is predicted very well.

Applications of the techniques to a coulomb-damped response are examined next. The response is generated numerically by integrating the following equation:

$$\ddot{x} + \omega_n^2 x + \mu\dot{x}/|\dot{x}| = 0 \tag{25}$$

where $\omega_n = 2\pi \times 9$ rad/s and $\mu = 300$. Estimated dampings with time are shown in Fig. 4. Here the analytical values of equivalent damping are obtained as

$$\zeta_{eq}(t) = 2\mu/\left[\pi\omega_n^2 a(0) - 2\mu\omega_n t\right] \tag{26}$$

It can be seen that both techniques are able to predict the proper damping characteristics from the transient response. Again, for this system the STD technique appears superior in spite of smaller block size. For the coulomb-damped case, the equivalent damping increases with decreasing amplitude, whereas for quadratic damping it decreases.

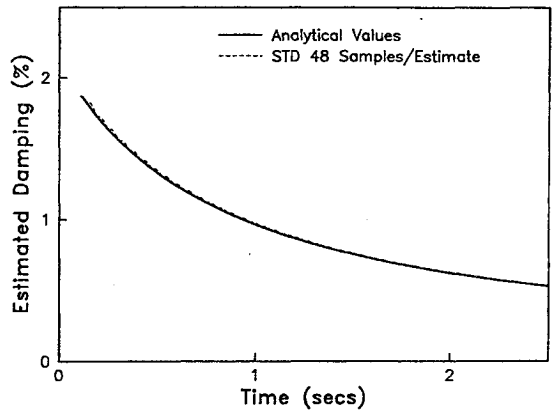

Fig. 3 Equivalent damping estimates for quadratic damping using sparse time domain method (data matrix size = 48 samples).

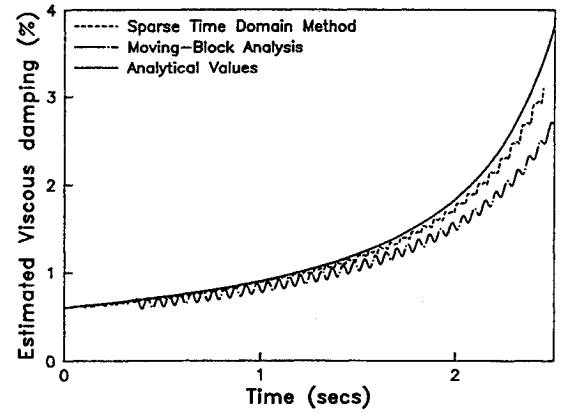

Fig. 4 Equivalent damping estimates for coulomb damping, using sparse time domain, data matrix = 48 samples and moving-block analysis, block size = 100 samples.

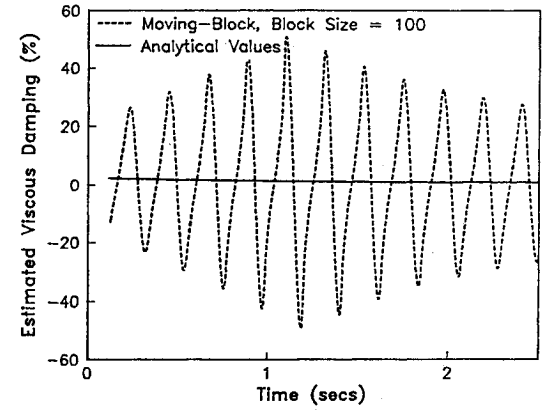

Fig. 5 Effect of undamped response on the estimation of equivalent damping for quadratic damping using moving-block analysis (frequency = 9 Hz, undamped mode = 13.6 Hz).

Effect of Close Modes

In a helicopter in forward flight, the periodic aerodynamic environment at the rotor disk leads to the generation of forces on the blade consisting of harmonics of the rotational frequency. The resulting undamped response may be simulated by the addition of an undamped sinusoid to transient response data. To investigate the effect of a forced response, an undamped sinusoid was added to a quadratically damped response and the damping was estimated using both the moving-block method and the STD technique. This undamped response is at 13.6 Hz, whereas the frequency of interest is 9 Hz. These frequencies are chosen to respectively represent the rotating speed and the lag-mode frequency of a particular Froude-scaled bearingless rotor model. The initial amplitudes of both modes are equal. In spite of the fact that the undamped mode is well separated from the frequency of interest, the moving-block results shown in Fig. 5 are significantly affected by the leakage from the undamped response. This shows up as a beat frequency of 4.6 Hz on the damping plot and obscures the correct trend. Because of the scaling, the time variation of the analytical equivalent damping is not clearly visible in this figure. Here a large leakage effect is a result of the small number of samples used to estimate the moving-block amplitudes.

Better results are obtained for this case by using the STD technique with fewer number of samples and the results are shown in Fig. 6. This is because time domain methods are not affected by leakage. For these results the data matrix Φ is chosen to be a square matrix. Two block sizes consisting respectively of 48 and 60 samples per block are selected. Although both block sizes essentially capture the damping trend, significant superimposed oscillations may be observed on the damping estimates obtained using 48 samples. Comparing with Fig. 3, which was also obtained using the 48 samples per block but without addition of the undamped sinusoid, one concludes that undamped response plays an important role in the identification of system damping. To examine the frequency contents of this damping plot, spectrum analysis of Fig. 6 is made and it is plotted in Fig. 7. It reveals certain dominating frequencies (18 and 36 Hz) at even multiples of the primary frequency. These frequencies are the frequency separations between the primary frequency (9 Hz) and its harmonics (27, 45 Hz, etc.). The oscillations are therefore caused by the linearization of the response within each block. This means that the nonlinearities are transformed into deterministic perturbations at harmonics in the linear solution. The characteristics of these perturbations then show up as fluctuations in estimated damping. From a previous study for linear viscous damping,[13] it was seen that the addition of an undamped response increased the sensitivity of the STD method to noise. For the case with nonlinear damping, the nonlinearities behave like noise in degrading the damping estimation and this explains the difference between Figs. 6 and 3. Therefore, to cover the influence of nonlinearities, one needs to include some of the singular values that would typically be associated with noise in Eq. (17). For example, for the case of quadratic damping, if two more singular values (equivalent to a mode) are

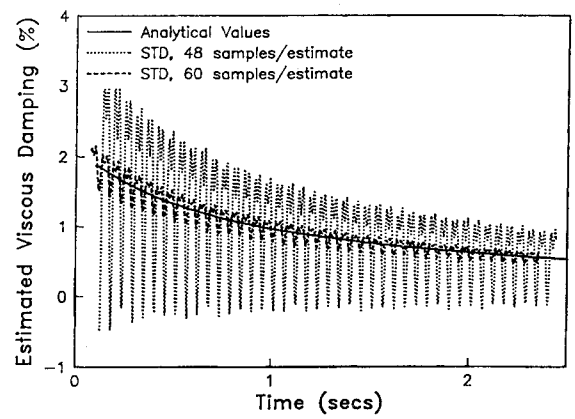

Fig. 6 Effect of undamped response on the estimation of equivalent damping for quadratic damping using sparse time domain method (frequency = 9 Hz, undamped mode = 13.6 Hz).

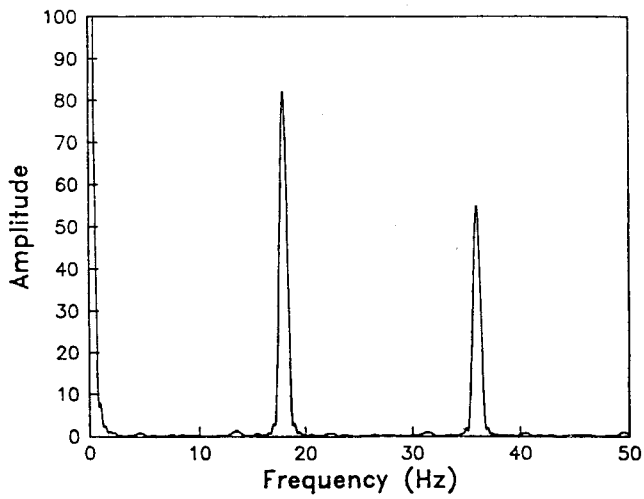

Fig. 7 Spectrum of equivalent damping estimates of quadratic damping using sparse time domain method (48 samples/estimate).

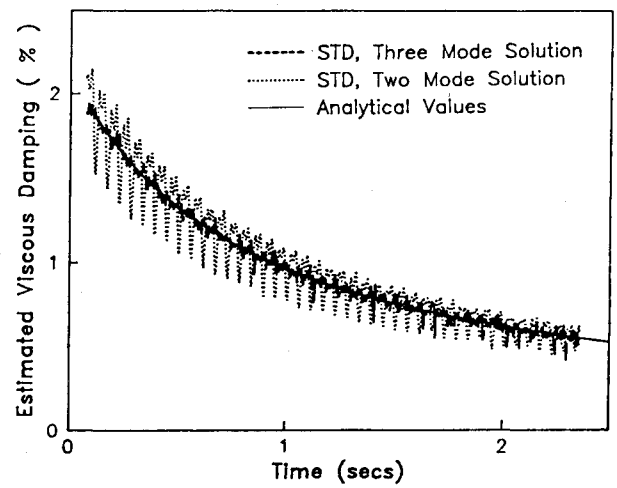

Fig. 8 Effect of additional mode on the estimation of equivalent damping for quadratic damping using sparse time domain method (60 samples/estimate, frequency = 9 Hz, undamped mode = 13.6 Hz).

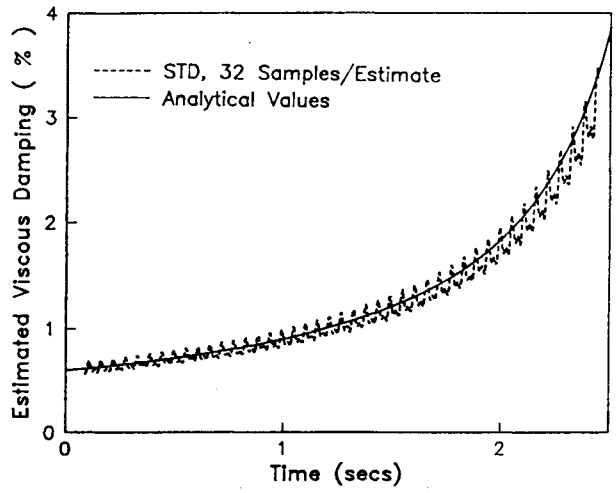

Fig. 9 Equivalent damping estimates for coulomb damping using sparse time domain analysis.

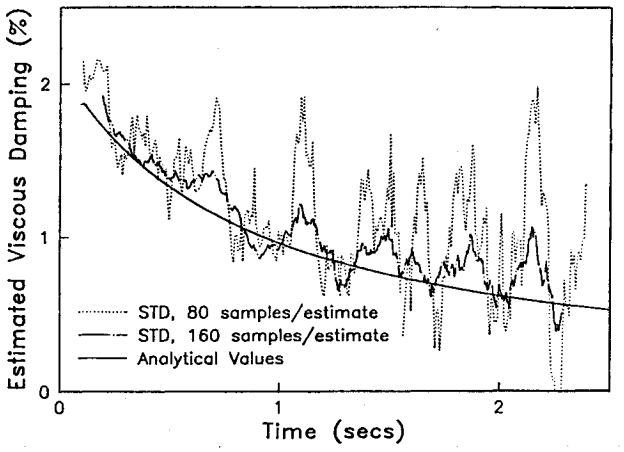

Fig. 10 Estimation of equivalent damping for quadratic damping using sparse time domain method (5% noise addition).

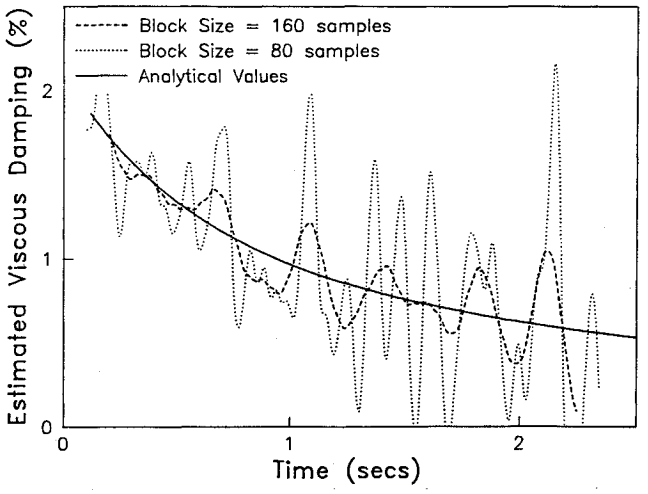

Fig. 11 Estimation of equivalent damping for quadratic damping using moving-block analysis (5% noise addition).

included in the estimation, the results are shown in Fig. 8. There is a considerable improvement in damping estimation by including an additional mode. It is however necessary to use caution when including these singular values. If the oscillations are random, then these are typically associated with noise; on the other hand, if the oscillations are deterministic dominated by a few frequencies, then these are generally caused by nonlinear damping behavior. In general, the perturbations on the estimates may be reduced by the use of a large block size with a large overlap between adjacent blocks (see Fig. 6).

Similar results such as in Fig. 6 may be obtained for coulomb damping. As an example, Fig. 9 shows damping estimates for coulomb damping without the addition of an undamped response. These are produced by analysis of a smaller data section (32 samples). Here it can be seen that superimposed oscillations occur in the regions of the response where amplitudes are small. This shows that the deterministic oscillations are not due to the undamped response but are amplified by it. It is important to note that the most nonlinear effects occur at low amplitudes for coulomb-damped systems and at high amplitudes for quadratically damped systems.

Effect of Noise

In the earlier results, there is no addition of noise to the response data. To determine the effect of noise on the identification techniques, zero-mean white noise with normal distribution is added to the quadratically damped response. Addition of the noise is based on the ratio of the standard deviation of the noise to the root-mean-square value of the response. Figure 10 shows the effect of 5% noise addition on the damping estimation with the STD method using 80 and 160 samples per damping estimate. There is a considerable error in the estimated values. In Fig. 11, damping estimates are shown for this case obtained by use of the moving-block analysis. Results are calculated using two block sizes consisting respectively of 60 and 160 samples. As expected, the accuracy of estimated values improve with larger block size. Comparison of Figs. 10 and 11 indicates that the estimates from both techniques are

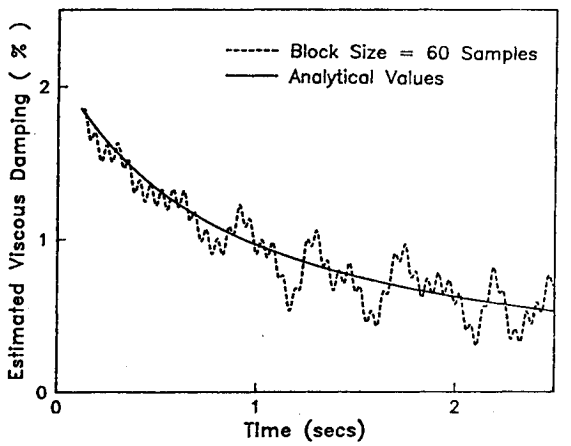

Fig. 12 Estimation of equivalent damping for quadratic damping using moving-block method and four averages of data (5% noise addition).

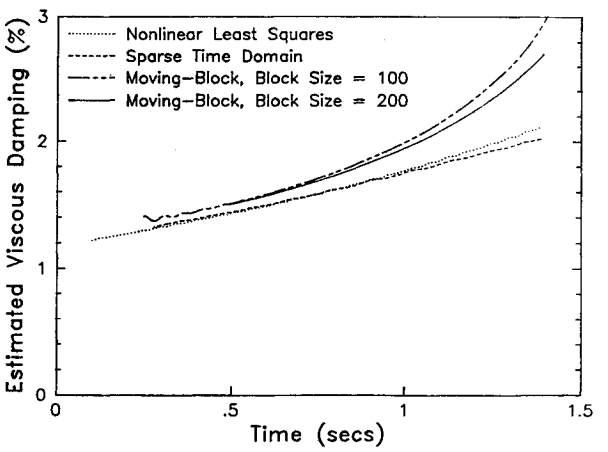

Fig. 13 Cumulative equivalent damping estimates for coulomb damping.

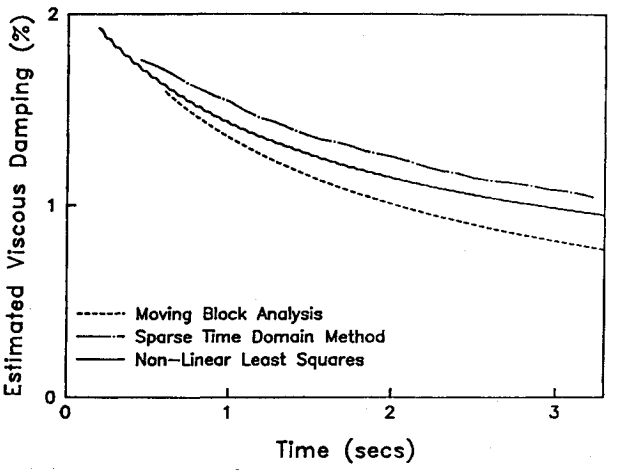

Fig. 14 Cumulative equivalent damping estimates for quadratic damping.

not good for a small block of data (80 samples). However, there is less randomness in the moving-block estimates. The estimates may be improved in two ways. First, if the damping is slowly varying with time as is the case here, a larger segment of the data improves the damping estimates. This would have the effect of smoothing the variations. As is shown in Figs. 10 and 11, increasing the block size from 80 to 160 samples considerably improves the damping estimate. However, with the larger block size, estimates close to the starting point of the data are lost. A second method is to average the data from identical experiments. This effect is illustrated in Fig. 12 for five averages, which when compared to Fig. 11 shows some improvement. This procedure however requires identical experiments.

Averaging Effect of Algorithms

It is customary to estimate only one damping value per transient response record. This value then represents (in some sense) the equivalent damping of the entire section of the response. It is of interest to know whether moving-block analysis and the STD method determine the same (cumulative) damping values for the same length of nonlinear transient response. Again two cases of nonlinear damping are examined. Figure 13 shows the estimated damping values for a coulomb-damped system, where the transient response is generated using Eq. (25) with $y(0) = 5$. A nonlinear least-square estimate of the equivalent damping is also shown in Fig. 13. This estimate is obtained by fitting the equation of a viscously damped single degree of freedom to the data. For results, the response up to a particular time is used to calculate the damping value that correpsonds to that time. Subsequent damping values are calculated by including more data points. It may be observed that both the moving-block analysis and the STD techniques produce different values of linear damping from the same duration of transient response record. The estimated damping values for quadratic damping are shown in Fig. 14. This again shows that damping values estimated by the two techniques can be quite different using the same amount of transient response record. This is less important for small data samples but becomes significant for longer records. Results for moving-block analysis are relatively insensitive to block size as can be seen from Fig. 15 in which the spectral amplitudes were obtained using three different block sizes. This does not contradict the behavior observed in Figs. 1a and 1b. In Fig. 15, all of the data up to a particular duration are used to produce one damping estimate. In Figs. 1a and 1b, only a few data points centered at a particular time are used to produce the corresponding damping estimate. The results of the STD method are quite sensitive to the way the total number of samples are

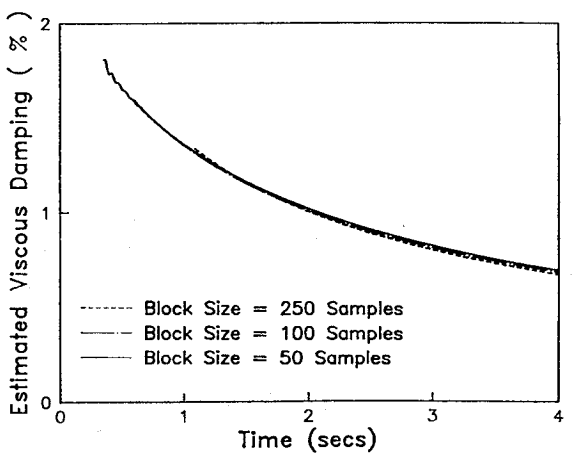

Fig. 15 Effect of block size on cumulative damping estimates for quadratic damping using moving-block analysis.

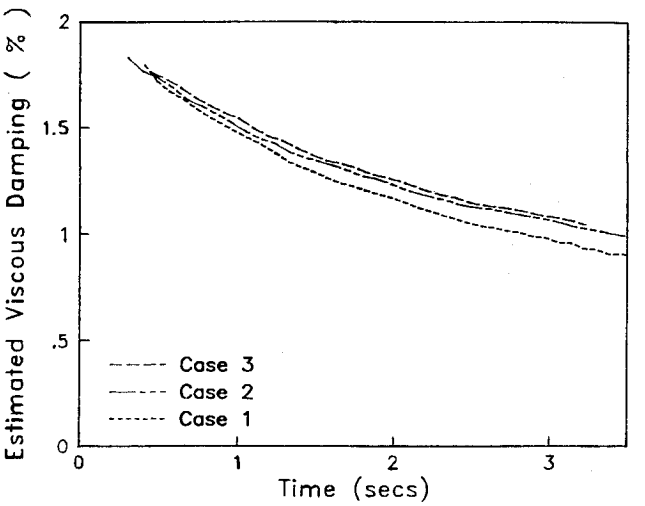

Fig. 16 Effect of data matrix arrangement on cumulative equivalent damping estimates for quadratic damping using sparse time domain method.

arranged in the data matrix (Fig. 16). The three cases studied for the time domain method are as follows:

1) In case 1, the number of rows and columns of the data matrix are the same, and adjacent rows and columns (in the data matrix) are shifted by four samples [i.e., $l = 4$, $p = 4$ in Eq. (15)]. This is also the case shown in Fig. 14.

2) Case 2 is the the same as case 1, except that the columns are shifted by eight samples and the rows by one sample.

3) In case 3, the data matrices have 30 more rows than columns, the column shift is eight samples, and the row shift is one sample.

These differences in the time domain technique are due to an empirically observed sensitivity to data matrix arrangement when noise is present in the data. This variation, however is not able to account for all of the differences in the estimates from the time domain and moving-block methods. The nonlinear least-squares estimate represents an attempt to define a cumulative damping estimate. It needs further investigation to obtain an unambiguous definition of equivalent viscous damping over several cycles that can be used for correlation studies.

Conclusions

Equivalent linear viscous damping characteristics for a system with nonlinear damping are identified from sampled, noise, multimode transient response data using modified versions of the moving-block analysis and sparse time domain technique. Data are simulated numerically to represent typical rotor environment. Two types of nonlinear dampings are studied, coulomb damping and quadratic damping. Based on this study the following conclusions are drawn.

1) It is necessary to use a Hanning window in the estimation of equivalent damping using a moving-block analysis to avoid large deviations of the estimates with small block sizes.

2) In the absence of noise and close modes, the sparse time domain method requires fewer samples than the moving-block method to accurately predict nonlinear damping characteristics.

3) The presence of a large undamped response may significantly affect the equivalent damping estimates obtained from either the moving-block analysis or the sparse time domain method. In the moving-block technique, the estimates get deteriorated by leakage effects, whereas in the modified sparse time domain method, perturbations caused by linearization are magnified.

4) Discrete frequency oscillations caused by nonlinearities may be reduced by including additional singular values/vectors in the singular value decomposition solution used with the sparse time domain method.

5) Measurement noise introduces random fluctuations in the damping estimates, and these can be minimized by averaging or by increasing the length of data for each damping estimate.

6) In processing the same length of nonlinear transient response record to obtain a damping value, estimates obtained by the moving-block method and the sparse time domain technique can be quite different even if signals are not polluted by noise.

References

[1]Warmbrodt, W., "Comparison of Experimental Rotor Damping Analysis," ITR Methodology Assessment Workshop, NASA and AVRADCOM, June 1983; also NASA CP 1007, 1988.

[2]Tomlison, G. R., "Detection, Identification and Quantification of Nonlinearity in Modal Analysis—A Review," *Proceedings of the 4th International Modal Analysis Conference,* Los Angeles, CA, Feb. 1986, Society for Experimental Mechanics, pp. 837–843.

[3]Nayfeh, A. H., "Parametric Identification of Nonlinear Dynamic Systems," *Computers and Structures,* Vol. 20, No. 1, 1985, pp. 487–493.

[4]Lai, H., "Development of Non-Linear Dynamic Data System (NLDDS) for On-Line Machining Vibratory System Characterization," Ph.D. Dissertation, Univ. of Wisconsin, Dept. of Mechanical Engineering, Madison, WI, 1984.

[5]Distefano, N., and Rath, A., "System Identification in Nonlinear Structural Seismic Dynamics," *Computer Methods in Applied Mechanics and Engineering,* Vol. 5, 1975, pp. 353–372.

[6]Yun, C., and Shinozuka, M. "Identification of Nonlinear Structural Dynamic Systems," *Journal of Structural Mechanics,* Vol. 8, No. 2, 1980, pp. 187–203.

[7]Leontaritis, I. J., and Billings, S. A., "Input-Output Parametric Models for Non-Linear Systems, Part II: Stochastic Non-Linear Systems," *International Journal of Control,* Vol. 41, No. 2, 1985, pp. 329–344.

[8]Masri, S. F., and Caughey, T. K., "A Non-Parametric Identification Technique for Nonlinear Dynamical Systems," *Journal of Applied Mechanics,* Vol. 46, No. 2, 1979, pp. 433–447.

[9]Udwadia, F. E., and Kuo, C. P., "Non-Parametric Identification of a Class of Nonlinear Close-Coupled Dynamic Systems," *Earthquake Engineering and Structural Dynamics,* Vol. 9, No. 4, 1981, pp. 385–409.

[10]Hadjian, A. H., Masri, S. F., and Saud, A. F., "A Review of Methods of Equivalent Damping Estimation from Experimental Data," *Journal of Pressure Vessel Technology,* Vol. 109, No. 2, 1987, pp. 236–243.

[11]Hammond, C. E., and Doggett, R. V., Jr., "Determination of Subcritical Damping by Moving Block/Randomdec Applications," NASA Symposium on Flutter Testing Techniques, NASA SP-415 Oct. 1975.

[12]Bousman, W. G., and Winkler, D. J., "Application of the Moving Block Analysis," *Proceedings of the AIAA/ASME/ASCE/AHS 22nd Structures, Structural Dynamics and Materials Conference,* AIAA, New York, 1981, pp. 755–763.

[13]Tasker, F., and Chopra, I., "Assessment of Transient Testing Techniques for Rotor Stability Testing," *Journal of the American Helicopter Society,* Vol. 35, No. 1, 1990, pp. 39–50.

[14]Wang, J. M., Chopra, I., Samak, D. K., and Green, M., "Theoretical and Experimental Investigation of the Aeroelastic Stability of an Advanced Bearingless Rotor in Hover and Forward Flight," AHS National Specialists' Meeting on Rotorcraft Dynamics, Arlington, TX, Nov. 13–14, 1989.

[15]Ibrahim, S. R., "An Upper Hessenberg Sparse Matrix Algorithm for Model Identification on Minicomputers," *Journal of Sound and Vibration,* Vol. 113, No. 1, 1987, pp. 47–57.

[16]Kumaresan, R., and Tufts, D., "Estimating the Parameters of Exponentially Damped Sinusoids and Pole Zero Modeling in Noise," *IEEE Transactions on Acoustics Speech and Signal Processing,* Vol. 30, No. 6, 1982, pp. 833–840.

[17]Hamming, R. W., *Numerical Methods for Scientists and Engineers,* McGraw-Hill, New York, 1973, pp. 546, 547.

[18]Stewart, W. J., and Jennings, A., "A Simultaneous Iteration Algorithm for Real Matrices," *ACM Transactions on Mathematical Software,* Vol. 7, No. 2, 1981, pp. 184–198.

[19]Minorsky, N., *Introduction to Non-Linear Mechanics,* J. W. Edwards, Ann Arbor, MI, 1947.

[20]Mendel, J. M., *Discrete Techniques of Parameter Estimation,* Marcel Dekker, New York, 1973.